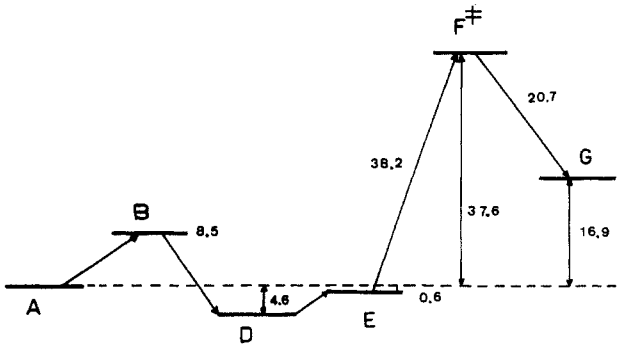

Figure 5. Relative energies among structures considered in the stepwise mechanism (MP2/6-31G*, estimated) (kcal/mol).

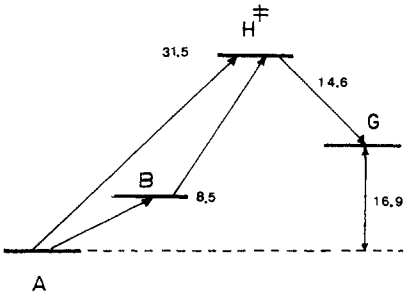

Figure 6. Relative energies among structures considered in the concerted mechanism (MP2/6-31G*, estimated) (kcal/mol).

MP4) are necessary in order to definitely conclude if the hydrogen transfer proceeds with or without transition state. The conformer D becomes slightly lower in energy than the conformer A, but it also can be changed with fully optimized geometries at higher levels of calculations.

As mentioned above, the H_m atom at the concerted transition state (H) is situated very near to the O atom. Therefore, it can be speculated that the dissociation of C_2–C_3 in (H) is more favorable than that in the transition state (F), due to a certain stability interaction in (H). At all levels of calculations the dissociation via the transition state (H) (concerted) takes place by about 3–6 kcal/mol lower than that in the stepwise pathway via the transition state (F).

Schematic diagrams for the relative energies among structures considered in the stepwise and concerted pathways of butanal cation and its fragments are shown in Figures 5 and 6, respectively.

4. Conclusion

The γ-hydrogen transfer to the double-bonded oxygen in the butanal cation is found to be an easy process, without or with a very small activation energy. Even at the concerted transition state, it is also transferred before the bond cleavage takes place. The difference between both transition states (F) and (H) is merely due to their different configurations. Therefore, it seems that the classification as concerted or stepwise is not quite justified with regard to the timing of the processes.

The rate-determining step of the McLafferty-type rearrangement reaction is found to be the dissociation of the species, cleavage of the C_2–C_3 bond in butanal cation in different configurations. The most favored rearrangement pathway is that satisfying the "preassociation mechanism", namely that via the transition state (H) in the present case.

Absolute Rate Constant and Branching Fractions for the H + HO_2 Reaction from 245 to 300 K

Leon F. Keyser

Jet Propulsion Laboratory, California Institute of Technology, Pasadena, California 91109
(Received: December 18, 1985; In Final Form: February 17, 1986)

The total rate constant and the branching fractions for the reactions H + HO_2 → OH + OH (k_{1a}), → O + H_2O (k_{1b}), → H_2 + O_2 (k_{1c}) have been determined by using resonance fluorescence detection of radical and atomic species. For the total rate constant measurement, pseudo-first-order conditions were used with HO_2 concentrations in large excess over initial atomic hydrogen. The result is (8.7 ± 1.5) × 10^{-11} cm^3 $molecule^{-1}$ s^{-1}, independent of temperature from 245 to 300 K. For the branching fraction measurements, product yields of OH and atomic oxygen were measured by adding HO_2 to an excess of atomic hydrogen. Atomic oxygen yields decreased when OH quenchers, such as water or CO, were added. A similar reduction in atomic oxygen yields was observed in the H + NO_2 reaction. Evidence is presented that the product yields observed with added water are free of interference from secondary reactions. The resulting branching fractions are k_{1a}/k_1 = (0.90 ± 0.04), k_{1b}/k_1 = (0.02 ± 0.02), and k_{1c}/k_1 = (0.08 ± 0.04), independent of temperature from 245 to 300 K.

Introduction

The reaction of atomic hydrogen with the hydroperoxyl radical has three possible exothermic reaction channels (eq 1). In the

$$H + HO_2 \rightarrow OH + OH \quad (1a)$$

$$H + HO_2 \rightarrow O + H_2O \quad (1b)$$

$$H + HO_2 \rightarrow H_2 + O_2 \quad (1c)$$

Earth's mesosphere and lower thermosphere (50 to 100 km), atomic hydrogen concentrations become large enough that each of these reaction paths becomes relatively important in the odd hydrogen (HO_x = H + OH + HO_2) chemistry of this region. Channel a contributes to OH radical production while channel c is an important source of molecular hydrogen. Reaction paths b and c compete with the OH + HO_2 reaction as the major losses of HO_x and, thus, limit the effectiveness of the HO_x radicals in destroying odd oxygen (O + O_3).[1-4] Besides its importance in the atmosphere, reaction 1 is of interest in combustion chemistry as a chain propagation step (channel a) and as chain termination steps (channels b and c).

(1) Allen, M.; Lunine, J. I.; Yung, Y. L. *J. Geophys. Res.* **1984**, *89*, 4841.
(2) Nicolet, M. In *Proceedings NATO Advanced Study Institute on Atmospheric Ozone: Its Variation and Human Influences*, Aiken, A. C., Ed.; U.S. Department of Transportation: Washington, DC, 1980; pp 823-864, FAA-EE-80-20.
(3) Prather, M. J. *J. Geophys. Res.* **1981**, *86*, 5325.
(4) Liu, S. C.; Donahue, T. M. *J. Atmos. Sci.* **1974**, *31*, 1118.

0022-3654/86/2090-2994$01.50/0

The total rate constant has been determined by several recent studies which used sensitive detection methods to monitor one or both reactants. Near 300 K values of k_1 range from 4.6×10^{-11} to 7.4×10^{-11} cm^3 molecule^{-1} s^{-1}.[5-7] Wide differences in the branching fractions have been found: reported values range from 0.05 to 0.87 for k_{1a}/k_1, from 0.02 to 0.52 for k_{1b}/k_1, and from 0.09 to 0.62 for k_{1c}/k_1, all near 300 K.[7-12] No previous study of the temperature dependence of k_1 or of the branching fractions has been reported.

In the present study, the absolute total rate constant and the branching fractions have been determined from 245 to 300 K by using resonance fluorescence detection of radical and atomic species. For the total rate constant measurement, pseudo-first-order conditions were used with [HO_2] >> [H]. The rate constant was determined directly from the slopes of ln [H] vs. time plots. For the branching fraction measurements, excess atomic hydrogen was used; k_{1a}/k_1 and k_{1b}/k_1 were determined from [OH] and [O] produced, respectively, per initial [HO_2]; k_{1c}/k_1 was then determined by difference.

Experimental Method

Low-Pressure Flow System. The discharge-flow system used in this study has been described in detail previously.[13,14] A dual-resonance fluorescence cell allowed simultaneous detection of two radical or atomic species. This greatly improved sensitivity and simplified comparison of experimental concentration vs. time profiles with those generated from computer simulations.

For the present study a 50.5-mm-diameter flow reactor was used. Temperatures in the range 245 to 300 K were maintained within ±2 K by passing a heat exchange fluid through a jacket which completely surrounded the tubular reactor. Total pressures in these experiments were between 1 and 2 Torr of helium.

All reactor surfaces were coated with a halocarbon wax (Series 15-00, Halocarbon Corp.). To check the stability of the surface condition, OH wall loss rates (k_w) were determined immediately before or after each series of runs. Without added NO, k_w ranged from approximately 2 to 15 s^{-1}; with NO, k_w was 5 to 30 s^{-1}. In the presence of NO, the reported k_w includes a small contribution from the reaction of OH and NO (see the discussion of OH detector calibrations below). With this wall coating HO_2 loss rates generally were less than 5 s^{-1}; atomic hydrogen and oxygen losses were less than 2 s^{-1}.

HO_2 Production and Detection. The HO_2 source has been described in detail previously.[15] HO_2 radicals were generated in a movable reactor by adding atomic fluorine to an excess of H_2O_2 (eq 14). Atomic fluorine was produced in a microwave

$$F + H_2O_2 \rightarrow HO_2 + HF \quad (14)$$

discharge of dilute mixtures of either F_2 or CF_4 in helium. In both cases an uncoated alumina discharge tube was used with maximum power less than 10 W. Typical dissociation efficiencies were 50% for F_2 and 4% for CF_4. This source was used to generate HO_2 concentrations in the main reaction zone between 3×10^{11} and 3×10^{12} cm^{-3}. Background concentrations of OH were generally about 1×10^{10} cm^{-3}. Atomic oxygen backgrounds ranged from 5×10^9 to 1.5×10^{10} cm^{-3} with typical values less than 10^{10} cm^{-3}. Atomic hydrogen was less than 10^9 cm^{-3}. Use of F_2 or CF_4 as the F atom precursor did not significantly alter the observed background concentrations.

Concentrations of HO_2 were determined by quantitatively converting it to OH with an excess of NO (eq 21). For the total

$$HO_2 + NO \rightarrow OH + NO_2 \quad (21)$$

rate constant measurement, NO was added at a fixed point approximately 3-ms upstream of the OH detector. Details of this method and the small corrections (less than 6%) for radical losses which are necessary to obtain absolute HO_2 concentrations have been discussed earlier.[13] For the branching fraction measurements, NO was added at several reaction times and a linear extrapolation to zero time was used to determine [HO_2]. Details of this method are discussed below.

Atomic Hydrogen Source. Atomic hydrogen was produced at a fixed point upstream of the main reaction zone by passing dilute mixtures of H_2 in helium through a microwave discharge operated at 50 W. An uncoated quartz discharge tube was used. Atomic hydrogen was generated at concentrations between about 1×10^{11} and 1×10^{13} cm^{-3} with background concentrations of both OH and atomic oxygen less than 1×10^{10} cm^{-3}.

Detector Calibrations. OH was monitored by resonance fluorescence near 308 nm. Known concentrations of OH were generated by reacting NO_2 with excess H atoms (eq 22).

$$H + NO_2 \rightarrow OH + NO \quad (22)$$

Calibrations were run both with and without added NO to account for the increased OH loss in the presence of NO. Corrections, about 5% or less, were made for OH losses due to disproportionation (eq 2). Additional corrections, typically less than 20%,

$$OH + OH \rightarrow O + H_2O \quad (2)$$

were made for OH wall loss and for combination with NO (eq 23) by using measured values for the total pseudo-first-order decay.

$$OH + NO + He \rightarrow HONO + He \quad (23)$$

Atomic oxygen was followed by resonance fluorescence near 130 nm. Oxygen atom concentrations were calibrated by adding a known amount of NO to an excess of N atoms (eq 43).

$$N + NO \rightarrow N_2 + O \quad (43)$$

Fluorescence signals were tested for linearity by fitting the data to the relation $I = a[O]^n$. For [O] less than 1.1×10^{11} cm^{-3}, $n = 0.98 \pm 0.01$; that is, the calibration was linear within 2% over the concentration range of interest.

Atomic hydrogen concentrations were monitored by resonance fluorescence at 121.6 nm. For [H] < 3×10^{12} cm^{-3}, atomic hydrogen signals were calibrated by converting the H atoms to OH by adding an excess of NO_2 (eq 22).[16] The OH fluorescence had been previously calibrated as described above. For [H] > 3×10^{12} cm^{-3}, atomic hydrogen signals were calibrated by titrating with NOCl; the 762-nm chemiluminescence of HNO was used to determine the endpoint.[17,18] At low concentrations, the atomic hydrogen data were tested for linearity by using the same method as described above for the atomic oxygen signals. For [H] < 1×10^{11} cm^{-3}, the calibration was linear within 5% ($n = 0.95 \pm 0.03$). No corrections to observed H atom decays were made for this effect because [H] < 6×10^{10} cm^{-3} at the shortest reaction times used with HO_2 added.

Absolute Reaction Times. Although absolute reaction times were not required for the total rate constant determination, they were needed to make corrections for secondary chemistry during the branching fraction measurements described below. Absolute

(5) Hack, W.; Preuss, A. W.; Wagner, H. Gg.; Hoyermann, K. *Ber. Bunsenges. Phys. Chem.* **1979**, *83*, 212.
(6) Thrush, B. A.; Wilkinson, J. P. T. *Chem. Phys. Lett.* **1981**, *84*, 17.
(7) Sridharan, U. C.; Qiu, L. X.; Kaufman, F. *J. Phys. Chem.* **1982**, *86*, 4569.
(8) Clyne, M. A. A.; Thrush, B. A. *Proc. R. Soc. London, Ser. A* **1963**, *275*, 559.
(9) Dodonov, A. F.; Lavrovskaya, G. K.; Tal'roze, V. L. *Kinet. Catal.* **1969**, *10*, 573.
(10) Bennett, J. E.; Blackmore, D. R. *Symp. (Int.) Combust., [Proc.], 13th* **1971**, 57.
(11) Westenberg, A. A.; deHaas, N. *J. Phys. Chem.* **1972**, *76*, 1586.
(12) Hack, W.; Wagner, H. Gg.; Hoyermann, K. *Ber. Bunsenges. Phys. Chem.* **1978**, *82*, 713.
(13) Keyser, L. F. *J. Phys. Chem.* **1982**, *86*, 3439.
(14) Keyser, L. F.; Choo, K. Y.; Leu, M. T. *Int. J. Chem. Kinet.* **1985**, *17*, 1169.
(15) Keyser, L. F. *J. Phys. Chem.* **1981**, *85*, 3667.
(16) Kleindienst, T. E.; Finlayson-Pitts, B. J. *Chem. Phys. Lett.* **1979**, *61*, 300.
(17) Clyne, M. A. A.; Stedman, D. H. *Trans. Faraday Soc.* **1966**, *62*, 2164.
(18) Clyne, M. A. A.; Thrush, B. A. *Discuss. Faraday Soc.* **1962**, *33*, 139.

times were determined by plotting ln ($[H]_0/[H]$) vs. relative times; here $[H]_0$ and [H] are atomic hydrogen concentrations in the absence and presence, respectively, of added HO_2. Zero intercepts of these plots were then used to calculate the absolute reaction times. Estimated errors in the absolute times are ±2 ms.

Reagents. Gases used were chromatographic grade helium (99.9999%), research grade hydrogen (99.9995%), ultrahigh-purity nitrogen (99.999%), nitric oxide (99.0%), research purity carbon monoxide (99.99%), CF_4 (99.9%), and a 0.5% mixture of F_2 in helium. The nitric oxide was purified by passage through a molecular sieve (13X) trap at 195 K. Nitrogen dioxide was prepared from nitric oxide as described earlier.[13] The fluorine in helium mixture was passed through a 77 K trap, and the chromatographic helium was passed through a molecular sieve (3A) trap at 77 K just prior to use. Carbon monoxide was purified by liquifying the gas at 77 K and then pumping the vapor through a molecular sieve (3A) trap at 195 K. So that a constant flow rate of carbon monoxide could be maintained, the 77 K trap was heated slightly by passing a stream of nitrogen gas through the liquid nitrogen. Hydrogen peroxide was obtained commercially and concentrated further by vacuum distillation. Vapor pressure measurements indicated that the final liquid-phase concentration was 90 to 95 wt %. Water vapor was added to the reaction mixture by passing a stream of helium through the liquid which was maintained at a constant temperature.

Total Rate Constant

Experimental Conditions. For the total rate constant measurements, excess HO_2 was added to atomic hydrogen. Concentrations of HO_2 were in the range 8×10^{11} to 2.5×10^{12} cm^{-3} with initial atomic hydrogen concentrations of 7.4×10^{10} to 1.5×10^{11} cm^{-3}. Initial stoichiometric ratios, $[HO_2]_0/[H]_0$, ranged from 9 to 32. Concentrations of H_2O_2 were 7×10^{12} to 4×10^{13} cm^{-3}. Temperatures were in the range 245 to 300 K at a total pressure of 1 Torr of helium.

Data Analysis. Under these conditions, the loss of atomic hydrogen is pseudo-first-order and may be written

$$k_+^{I} = -(\mathrm{d} \ln [H]/\mathrm{d}t)_+ = k_1[HO_2] + k_-^{I} \qquad (I)$$

where k_+^{I} is the pseudo-first-order rate constant for loss of atomic hydrogen with HO_2 added to the system. Values of k_+^{I} were determined from the slopes of ln [H] vs. t plots with the F_2 discharge on. The term, k_-^{I}, describes all H atom losses other than reaction with HO_2; it includes, for example, reactions with H_2O_2 and F_2 and was determined experimentally from the slopes of ln [H] vs. t plots with the F_2 discharge off. This procedure for determining k_-^{I} overestimated the H + F_2 loss which occurred during the H + HO_2 measurement (F_2 discharge on) when approximately 50% of the F_2 was dissociated. However, the total H atom loss with the discharge off was small (typically k_-^{I} was less than 5% of k_+^{I}) and k_-^{I} was not corrected for the dissociation of F_2 because of the uncertainty in separating the H + F_2 loss from other possible loss terms.

Results. Atomic hydrogen decays for several HO_2 concentrations at 260 K are shown in Figure 1. No evidence of curvature was observed in the plots over the 8- to 25-ms time interval used. Slopes of these plots were used to determine ($k_+^{I} - k_-^{I}$). Losses observed in the absence of HO_2 (k_-^{I}) generally were less than 5% of k_+^{I}. Table I summarizes the total rate constant experiments. Concentrations of HO_2 given in column 3 are the average of the concentrations observed at the minimum and maximum reaction times of each run. The total observed HO_2 decays due to wall loss, disproportionation (eq 7), and reaction with atomic hydrogen averaged less than 20%. Corrections (less than 6%) for radical losses during the HO_2 to OH conversion have been applied to the HO_2 concentrations.[13] Observed first-order rate constants were corrected for axial and radial diffusion (less than 18%) by using eq II, where D_c is the diffusion coefficient for atomic hydrogen

$$k^{I}_{corr} = k^{I}_{obsd}[1 + k^{I}_{obsd}(D_c/\bar{v}^2 + a^2/48D_c)] \qquad (II)$$

in helium, a is the tube radius, and $\bar{v}$ is the average flow velocity.[19,20] For these corrections a value of 2100 cm^2 s^{-1} was used

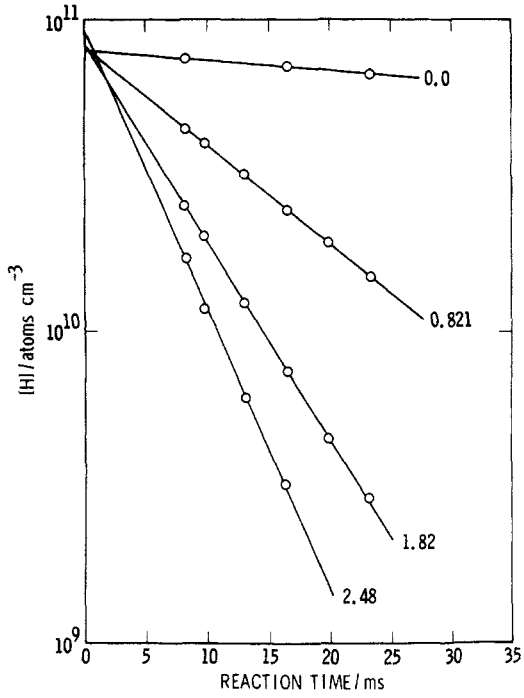

Figure 1. Pseudo-first-order decays of atomic hydrogen at 260 K. The numbers adjacent to each decay curve give $[HO_2]$ in units of 10^{12} cm^{-3}. The lines through the data points are linear least-squares fits.

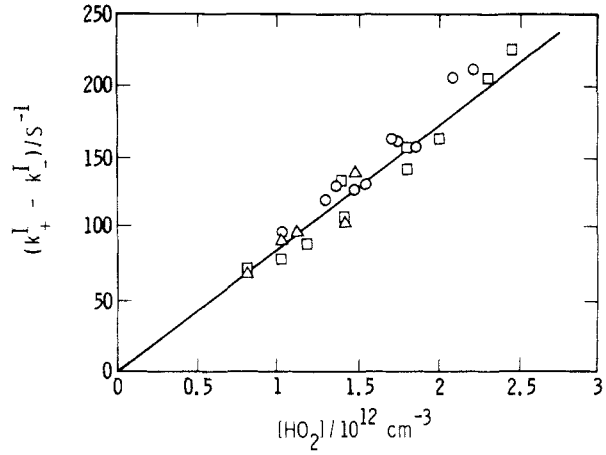

Figure 2. Pseudo-first-order rate constant vs. $[HO_2]$ from 245 to 300 K. The line through the data points represents the temperature-independent average: ○, 300 K; □, 260 K; △, 245 K.

for the diffusion coefficient at 300 K and 1 Torr.[21] Corrections due to the viscous pressure drop between the reaction zone and the pressure measurement port[22] were negligible (less than 1%). Net corrections to k_1 due to radical losses and diffusion ranged from −3% to +13% with an average value of +4% which is well within the overall estimated experimental error of ±20%.

The last column of Table I gives the values for the bimolecular rate constant, k_1, obtained from $(k_+^{I} - k_-^{I})/[HO_2]$. Values for k_1 were also calculated from the slopes of $(k_+^{I} - k_-^{I})$ vs. $[HO_2]$ plots and the results are given in Table II and Figure 2. Comparison of columns 2 and 3 of Table II shows no significant difference in k_1 obtained by either method; values obtained from the averages will be used in the rest of this discussion.

At the high initial stoichiometric ratios used in these experiments, secondary reactions are not expected to interfere. This is confirmed by the absence of curvature in atomic hydrogen pseudo-first-order decay plots and by the lack of any significant

(19) Brown, R. L. *J. Res. Natl. Bur. Stand. (U.S.)* **1978**, *83*, 1.
(20) Keyser, L. F. *J. Phys. Chem.* **1984**, *88*, 4750.
(21) Marrero, T. R.; Mason, E. A. *J. Phys. Chem. Ref. Data* **1972**, *1*, 3.
(22) Kaufman, F. *Prog. React. Kinet.* **1961**, *1*, 1.

TABLE I: Total Rate Constant Data[a]

temp, K	$\bar{v}$, cm s^{-1}	$10^{-12}[HO_2]$, cm^{-3}	$10^{-10}[H]$, cm^{-3}	$(k_+^I - k_-^I)$, s^{-1}	$10^{11}k_1$, cm^3 $molecule^{-1}$ s^{-1}
300	1535	1.04	11.0	97.1	9.34
		1.30	11.6	120.	9.23
		1.37	12.8	130.	9.49
		1.48	9.00	127.	8.58
		1.55	10.9	130.	8.39
		1.73	10.0	161.	9.31
		1.77	13.9	160.	9.04
		1.87	14.2	157.	8.40
		2.10	9.34	206.	9.81
		2.23	10.3	211.	9.46
					av = 9.10 ± 0.49[b]
260	1480	0.821	8.06	72.0	8.77
		1.03	7.42	79.0	7.67
		1.19	9.94	89.9	7.56
		1.41	8.46	134.	9.50
		1.42	11.5	108.	7.61
		1.82	7.99	156.	8.57
		1.82	10.1	141.	7.75
		2.01	11.0	163.	8.11
		2.33	10.6	204.	8.76
		2.48	7.78	225.	9.07
					av = 8.34 ± 0.69[b]
245	1345	0.828	9.12	67.3	8.13
		1.02	9.23	91.0	8.92
		1.12	10.0	98.3	8.78
		1.43	8.99	105.	7.34
		1.49	9.72	138.	9.26
					av = 8.49 ± 0.76[b]

[a] Total pressure was 1.0 Torr of helium. HO_2 was produced from the F + H_2O_2 reaction with F_2 as the source of F atoms. [b] Errors given are one standard deviation.

TABLE II: Total Rate Constant for the H + HO_2 Reaction

	$10^{11}k_1$, cm^3 $molecule^{-1}$ s^{-1}		
temp, K	average[a,b]	slope[a,c]	intercept,[a,c] s^{-1}
300	9.10 ± 0.49	9.71 ± 0.81	−10 ± 14
260	8.34 ± 0.69	9.19 ± 0.64	−13 ± 11
245	8.49 ± 0.76	8.37 ± 2.2	+1 ± 26
245 to 300	8.67 ± 0.70	9.32 ± 0.48	−9 ± 8

[a] Errors are one standard deviation. [b] From average of individual $(k_+^I - k_-^I)/[HO_2]$ values. [c] From plot of $(k_+^I - k_-^I)$ vs. $[HO_2]$.

variation in k_1 over a wide range of initial concentrations.

The observed rate constant appears to decrease slightly at lower temperatures. However, the standard deviation, σ, of the data is sufficiently large that, at the 95% confidence level ($\pm 2\sigma$), the data must be considered independent of temperature over the range studied. The results are summarized in row 4 of Table II. The value reported here for k_1 is $(8.7 \pm 1.5) \times 10^{-11}$ cm^3 $molecule^{-1}$ s^{-1}, independent of temperature over the range 245 to 300 K. The error given includes the standard deviation obtained from the data analysis plus an estimate of the experimental error.

Branching Fractions

Experimental Conditions. To determine the product yields of OH and atomic oxygen from reaction 1, excess atomic hydrogen was added to HO_2. Product concentrations were determined at reaction times from 5 to 20 ms. Initial concentrations of HO_2 were determined by adding excess NO to quantitatively convert it to OH. Atomic hydrogen concentrations were in the range 7×10^{12} to 1.2×10^{13} cm^{-3} with HO_2 in the range 2.8×10^{11} to 5.9×10^{11} cm^{-3}. Concentrations of NO were between 1.6×10^{14} and 2.2×10^{14} cm^{-3}. Hydrogen peroxide concentrations were 1.5×10^{12} to 2.5×10^{12} cm^{-3}. Temperatures were in the range 245 to 300 K with total pressures from 1 to 2 torr of helium.

Data Analysis. At the concentrations of atomic hydrogen or NO used in the present experiments, 95% of the initial HO_2 is removed within 3 to 5 ms by reactions 1 or 21, respectively. After this initial rapid removal of HO_2, product OH and atomic oxygen reach a quasi-steady-state and any further changes in [OH] and [O] over the time interval 5 to 20 ms are due to secondary chemistry involving long-lived species. The most important loss or source terms of this type include the following reactions:

$$OH + OH \rightarrow O + H_2O \quad (2)$$

$$O + OH \rightarrow H + O_2 \quad (3)$$

$$OH + H_2O_2 \rightarrow HO_2 + H_2O \quad (6)$$

$$OH + \text{wall} \rightarrow \text{products} \quad (18)$$

$$O + \text{wall} \rightarrow \text{products} \quad (20)$$

$$OH + NO + He \rightarrow HONO + He \quad (23)$$

Branching fractions can be obtained from concentrations of HO_2, OH, and O which are observed at a given reaction time. This point-by-point method assumes that the secondary chemistry can be neglected or that corrections for it can be made by calculation and separate experimental tests. This is the approach used in an earlier study by Sridharan et al.[7] and will be discussed more fully below.

In the present study, branching fractions were obtained from concentrations of HO_2, OH, and atomic oxygen which were corrected for secondary chemistry by using an internal experimental method. The slope of a linear least-squares fit of the data in the quasi-steady-state region (5 to 20 ms) was used to determine the net loss or production of OH and O atoms. Concentrations of HO_2, OH, and atomic oxygen which would have been observed in the absence of secondary chemistry were then determined by extrapolating to zero reaction time. This correction procedure was checked by using computer simulations which are discussed in detail below. Equations III and IV were then used to calculate

$$k_{1a}/k_1 = [OH]_0/2[HO_2]_0 \quad (III)$$

$$k_{1b}/k_1 = [O]_0/[HO_2]_0 \quad (IV)$$

the branching fractions for the a and b channels. The value for channel c was then determined by difference.

Results without Added OH Quenchers. Product yields observed in the absence of OH quenchers are discussed in the present section. The effects of added quenchers will be examined in the sections which follow. Typical experimental plots obtained when

TABLE III: H + HO_2 Branching Fraction Data without Added Quenchers[a]

temp, K	$10^{-11}[HO_2]_0$,[b] cm^{-3}	$10^{-12}[H]$, cm^{-3}	$(k_{1a}/k_1) = [OH]_0/2[HO_2]_0$[c,e]	$(k_{1b}/k_1) = [O]_0/[HO_2]_0$[d,e]
300	3.34	7.08	0.90 ± 0.05	0.08 ± 0.03
	3.92	4.35	0.77 ± 0.06[f]	0.06 ± 0.03[f]
	4.28	9.15	0.91 ± 0.04	0.1 ± 0.02
	4.32[g]	9.84	0.88 ± 0.02	0.07 ± 0.02
	4.95	7.02	0.93 ± 0.06	0.09 ± 0.01
	5.22	7.78	0.89 ± 0.04	0.09 ± 0.02
	5.36	10.1	0.84 ± 0.03	0.08 ± 0.01
	5.58[g]	11.2	0.88 ± 0.02	0.08 ± 0.01
			av = 0.89 ± 0.03	av = 0.08 ± 0.01
260	3.93	9.84	0.92 ± 0.03	0.08 ± 0.02
	4.42	9.31	0.92 ± 0.06	0.09 ± 0.02
	4.64	7.88	0.87 ± 0.02	0.08 ± 0.01
	5.43	9.82	0.90 ± 0.02	0.09 ± 0.01
	5.94	9.18	0.91 ± 0.02	0.09 ± 0.01
			av = 0.90 ± 0.02	av = 0.09 ± 0.01
245	4.61	9.46	0.88 ± 0.02	0.07 ± 0.02

[a] All experiments were at 1 Torr of helium with $[H_2O_2] < 2.5 \times 10^{12}$ cm^{-3} and $[H_2O] < 2 \times 10^{12}$ cm^{-3}. [b] HO_2 was produced from the F + H_2O_2 reaction; and unless otherwise indicated, F atoms were generated in a microwave discharge of F_2 plus helium. HO_2 was determined after quantitatively converting it to OH by adding excess NO. [c] Obtained by extrapolating $[OH]_t/2[HO_2]_0$ to $t = 0$. [d] Obtained by extrapolating $[O]_t/[HO_2]_0$ to $t = 0$. [e] Errors are one standard deviation. [f] This result not used in averages because of low [H], see text. [g] For these experiments, F atoms were generated from CF_4.

excess atomic hydrogen was added to HO_2 are shown in Figure 3 where the open symbols give the results without added quenchers. In figure 3 the relative yields $[OH]_t/2[HO_2]_0$ and $[O]_t/[HO_2]_0$ are plotted vs. reaction time. $[OH]_t$ and $[O]_t$ are the concentrations of OH and atomic oxygen observed at time, t. $[HO_2]_0$ is the concentration of HO_2 at zero reaction time; it was determined from a separate plot of $[OH]_t$ vs. t where in this case OH was produced from the reaction of HO_2 with excess NO. Concentrations of HO_2, OH, and atomic oxygen were corrected for background OH and atomic oxygen in the H atom and HO_2 sources. These background concentrations were also extrapolated to zero reaction time before the corrections were applied. For HO_2 and OH, background OH corrections averaged less than 5%; for atomic oxygen, the average background correction was 25%. Generally plots of OH yields vs. t were linear and decreased only slightly over the time interval observed. Similar behavior was observed in the case of atomic oxygen at 300 K. However, at temperatures below 300 K, atomic oxygen yields increased rapidly between 5 and 8 ms before reaching a quasi-steady-state at longer reaction times. Only the steady-state yields were used in the present determination.

The branching fraction measurements without added quenchers are summarized in Table III. The errors given for each measurement include uncertainties introduced by the extrapolation to time zero and uncertainties in the background corrections. The extrapolation error is taken to be one standard deviation of the $t = 0$ axis intercept and the background error is estimated to be one-half of the total background correction.

The results are independent of the initial atomic hydrogen concentration at or above 7×10^{12} cm^{-3}. This is evidence that no significant O atom or OH losses occurred during the H + HO_2 reaction. These losses would be due to reactions such as OH + HO_2 and O + HO_2. At lower atomic hydrogen concentrations, reaction times become sufficiently long that significant losses can occur. This was also demonstrated by the computer simulations discussed below. One experiment at an initial atomic hydrogen concentration of 4.35×10^{12} cm^{-3} yielded branching fraction results which are significantly lower; these were not included in the averages reported.

The branching fraction results are also independent of whether CF_4 or F_2 was used as the atomic fluorine source. This shows that the secondary chemistry associated with the fluorine source does not interfere with the present measurements since different impurities and different reaction products are present in each source.

No significant variation in the branching fractions was observed over the temperature range 245 to 300 K. The temperature-independent averages are $k_{1a}/k_1 = 0.89 \pm 0.02$ and $k_{1b}/k_1 = 0.08 \pm 0.01$. The errors given are one standard deviation obtained by averaging the individual measurements.

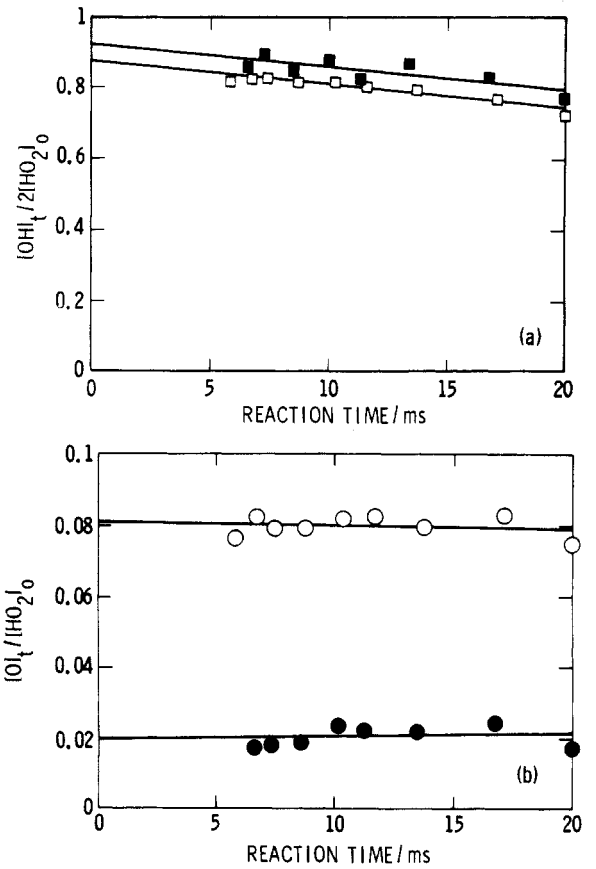

Figure 3. Product yields from H + HO_2 at 300 K. Open symbols are without added water; filled symbols are with water at a concentration of 4.9×10^{15} cm^{-3}. The lines through the data points are linear least-squares fits: (a) OH, (b) atomic oxygen.

Vibrationally Excited OH. Extrapolation of the product yields to zero reaction time corrects for secondary reactions which occur over the observational time interval of 5 to 20 ms. However, this procedure does not correct for secondary reactions associated with short-lived species. Such reactions could occur at times less than 5 ms and cannot be directly observed in the present experiments. Possible interference from short-lived species such as vibrationally

excited OH is discussed here and in the section which follows.

Reaction path 1a is sufficiently exothermic (36.8 kcal mol^{-1}) that vibrationally excited OH could be formed up to the $v = 3$ level. Indeed, production of excited OH from reaction 1a has been reported previously in studies of H + O_2 systems. Using the discharge-flow chemiluminescence detection technique, Charters and Polanyi[23] observed emission due to OH in the $v = 3$, 2, and 1 levels. They interpreted their results using a reaction mechanism in which HO_2 was formed from the H + O_2 + M reaction with subsequent production of vibrationally excited OH from reaction 1a. Using a similar experimental technique, Choo and Leu[24] also observed emission from the $v = 3$ and 2 vibrational levels of OH produced in H + O_2 systems. Neither study reported yields for the production of vibrationally excited OH.

In the present experiments, any vibrationally excited OH produced in reaction 1a was lost very rapidly due mainly to nonreactive quenching by atomic hydrogen (eq 33a, $k_{33a} = 3 \times$

$$OH^* + H \rightarrow OH + H \quad (33a)$$

10^{-10} cm^3 $molecule^{-1}$ s^{-1} [25]). Wall deactivation of OH* played only a minor role since the collision efficiency on a halocarbon-coated surface has been found to be approximately 2×10^{-3} which is much lower than on an acid-coated surface.[25] Despite the rapid loss by H atom quenching, reaction of OH* with atomic hydrogen (eq 33b), with OH itself (eq 34), or with atomic oxygen (eq 38)

$$OH^* + H \rightarrow O + H_2 \quad (33b)$$

$$OH^* + OH \rightarrow O + H_2O \quad (34)$$

$$OH^* + O \rightarrow H + O_2 \quad (38)$$

could conceivably interfere with the branching fraction measurements if the OH* rate constants are considerably higher than the ground-state values and if the yield of OH* from reaction 1a is sufficiently high. (Here OH* represents OH in the $v = 1$, 2, or 3 vibrational level of the ground electronic state.) At the atomic hydrogen concentrations used, the time to remove 95% of initial HO_2 by reaction 1 was less than 5 ms and the time to remove 95% of OH* by nonreactive quenching alone (eq 33a) was less than 2 ms. Thus, before the start of the observations at 5 ms, the secondary chemistry directly due to OH* would be essentially complete and corrections for it could not be made by the extrapolation procedure described earlier.

Results with Added OH Quenchers. To test for interference from vibrationally excited OH, quenchers such as water vapor and CO were added separately to several branching fraction measurements. Water vapor removes OH* by nonreactive quenching (eq 36).[26] In order to compete with atomic hydrogen

$$OH^* + H_2O \rightarrow OH + H_2O \quad (36)$$

quenching of OH*, water vapor was added at concentrations near 5×10^{15} cm^{-3}. Under these conditions, the time required to remove 95% of OH* by reaction 36 is less than 0.1 ms compared to about 2 ms for removal by atomic hydrogen quenching (eq 33a). A hydrogen-bonded complex of HO_2 and water vapor has been proposed[27] to account for the increase observed in some HO_2 reaction rates when water is added. However, the equilibrium constant for complex formation has been found to be about 3×10^{-19} cm^3 $molecule^{-1}$.[28] Thus, at the concentrations of HO_2 and water used in the present study, concentrations of the complex should be less than 3×10^9 cm^{-3} and can be neglected.

Water vapor was added over the temperature range 245 to 300 K. Typical experimental plots are shown in Figure 3 where the filled symbols represent yields with added H_2O. A small (possibly not a significant) increase was observed in OH yields. However, atomic oxygen yields were reduced by factors of about 2 to 4 when water vapor was present. The results are summarized in Table IV.

TABLE IV: H + HO_2 Branching Fraction Data with Added Quenchers[a]

temp, K	$10^{-11} \times [HO_2]_0$,[b] cm^{-3}	$10^{-12} \times$ [H], cm^{-3}	$(k_{1a}/k_1) = [OH]_0/2[HO_2]_0$[c,e]	$(k_{1b}/k_1) = [O]_0/[HO_2]_0$[d,e]
Water Vapor Added; $[H_2O] = 4.9 \times 10^{15}$ cm^{-3}; $p = 1$ Torr				
300	3.93	11.3	0.93 ± 0.05	0.01 ± 0.02
300	4.12	10.8	0.92 ± 0.04	0.02 ± 0.02
260	3.98	11.5	0.92 ± 0.04	0.03 ± 0.02
245	2.76	12.2	0.89 ± 0.07	0.04 ± 0.02
			av = 0.92 ± 0.02	av = 0.02 ± 0.01
Carbon Monoxide Added; $[CO] = 1.9 \times 10^{16}$ cm^{-3}; $p = 2$ Torr				
300	4.76	11.0		0.04 ± 0.02

[a] Footnotes are as in Table III.

TABLE V: Effect of OH Quenchers on Atomic Oxygen Yields from H + NO_2[a]

quencher added	quencher concn, cm^{-3}	$100[O]_0/[NO_2]_0$[b,c]
none		4.5 ± 0.4
H_2O	4.9×10^{15}	0.3 ± 0.2
CO	1.9×10^{16}	0.8

[a] All experiments were at 300 K. [b] Obtained by extrapolating $100 \cdot [O]_t/[NO_2]_0$ to $t = 0$. [c] Errors are one standard deviation.

Carbon monoxide removes OH* by nonreactive quenching (eq 44a) and by reaction (eq 44b) ($k_{44} = 8.3 \times 10^{-13}$ cm^3 $molecule^{-1}$

$$OH^* + CO \rightarrow OH + CO \quad (44a)$$

$$OH^* + CO \rightarrow H + CO_2 \quad (44b)$$

s^{-1} [29]). Carbon monoxide was added to branching ratio runs at 300 K only. Concentrations of CO were near 2×10^{16} cm^{-3}. Under these conditions, OH* was 95% removed by reactions 44a and 44b in less than 0.2 ms. With CO present atomic oxygen yields were reduced by about a factor of 2. The results are also given in Table IV.

With added quenchers, data analysis was the same as described above. Observed products were corrected for background concentrations in the atomic hydrogen and HO_2 sources; yields were then obtained by extrapolating to zero reaction time. However, because of the lower atomic oxygen yields, signal to noise levels were lower and background corrections were considerably higher for this species. Atomic oxygen background corrections with added quenchers averaged less than 60%, while for HO_2 and OH, they remained less than 5%. Calibrations of both OH and atomic oxygen resonance fluorescence signals were carried out at the concentrations of water and CO used in these experiments.

The large reduction in atomic oxygen yields with added OH quenchers suggests that a large fraction of the atomic oxygen observed in the H + HO_2 system without added quenchers is produced by secondary reactions involving vibrationally excited OH. The small increase in OH yields under these same conditions is also consistent with interference from reactions of OH*.

Since OH* could not be observed directly in the present experiments, it is difficult to tell whether addition of quenchers has completely eliminated interference from reactions of OH*. To test the effectiveness of the quenchers, the reaction of atomic hydrogen with NO_2 (eq 22) was used as an experimental model.

$$H + NO_2 \rightarrow OH^* + NO \quad (22)$$

This reaction is known to produce vibrationally excited OH in the $v = 1$, 2, and 3 states with yields from 40 to 50%.[25,30-34]

(23) Charters, P. E.; Polanyi, J. C. *Can. J. Chem.* **1960**, *38*, 1742.
(24) Choo, K. Y.; Leu, M. T., to be submitted for publication.
(25) Spencer, J. E.; Glass, G. P. *Chem. Phys.* **1976**, *15*, 35.
(26) Glass, G. P.; Endo, H.; Chaturvedi, B. K. *J. Chem. Phys.* **1982**, *77*, 5450.
(27) (a) Hamilton, E. J., Jr. *J. Chem. Phys.* **1975**, *63*, 3682. (b) Hamilton, E. J., Jr.; Lii, R. R. *Int. J. Chem. Kinet.* **1977**, *9*, 875.
(28) Lii, R. R.; Sauer, M. C., Jr.; Gordon, S. *J. Phys. Chem.* **1981**, *85*, 2833.
(29) Smith, I. W. M.; Williams, M. D. *Ber. Bunsenges. Phys. Chem.* **1985**, *89*, 319.

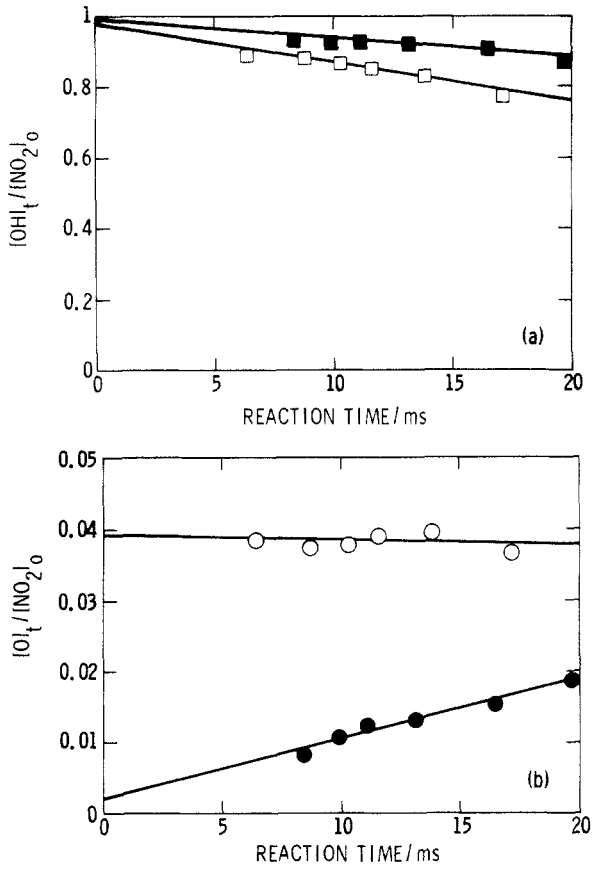

Figure 4. Product yields from H + NO_2 at 300 K. Open symbols are without added water; filled symbols are with water at a concentration of 4.9×10^{15} cm^{-3}. The lines through the data points are linear least-squares fits: (a) OH, (b) atomic oxygen.

Typical plots of product OH and atomic oxygen from reaction 22 are shown in Figure 4 where the filled and open symbols give the yields with and without added water vapor, respectively. Results of several experiments are summarized in Table V. The effect of quenchers on absolute OH yields from H + NO_2 cannot be observed since OH concentrations are obtained by setting $[OH]_0 = [NO_2]$ added. However, plots of OH yields vs. time (Figure 4a) show that the secondary loss of OH changed very little when water was added. Without OH quenchers, yields of atomic oxygen were quasi-steady-state in the time interval 5 to 20 ms and ranged from about 4 to 5%, independent of atomic hydrogen concentrations from 6×10^{12} to 1.2×10^{13} cm^{-3}. Similar atomic oxygen yields from H + NO_2 have been reported previously.[35,36] When quenchers were added, atomic oxygen concentrations were no longer steady state but increased over the reaction times observed. Yields determined by extrapolating to zero reaction time were less than 1% in the presence of OH quenchers.

Sufficient energy is not available to generate atomic oxygen as a primary product of the H + NO_2 reaction. Moreover, the 4 to 5% yields without added quenchers are much larger than expected from secondary reactions involving only ground-state OH. Thus, the major source of atomic oxygen in this system is most likely reactions of vibrationally excited OH such as OH* + H (eq 33b) or OH* + OH (eq 34). This is discussed in more detail in the computer simulation section which follows.

Addition of water to the H + NO_2 reaction system reduced atomic oxygen yields to less than 0.5%. This is evidence that addition of this quencher at the concentrations used effectively eliminated interference from vibrationally excited OH. Thus, any residual atomic oxygen observed in the H + HO_2 system with added water could not be due to secondary production from reactions of vibrationally excited OH but must have been a primary product of the H + HO_2 reaction itself. Carbon monoxide appears to be slightly less effective than water in reducing atomic oxygen yields in both the H + HO_2 and H + NO_2 systems. The results with added CO confirm the observations that atomic oxygen yields are sensitive to added OH quenchers. Since only a limited number of runs were carried out, they will not be discussed further here.

The discussion above shows that the branching fraction results with added water should be free of interference from secondary reactions. For the OH channel, k_{1a}/k_1 is independent of temperature. Its average with added water is 0.92 ± 0.02 and is not significantly different from the value of 0.89 ± 0.02 observed without added water. The combined average with and without added water is 0.90 ± 0.02. For the atomic oxygen channel, k_{1b}/k_1 with added water varies from 0.02 ± 0.02 at 300 K to 0.04 ± 0.02 at 245 K. This variation is not significant even at the 1σ level and only the temperature-independent average of 0.02 is reported. In summary the branching fractions reported here are $k_{1a}/k_1 = 0.90 \pm 0.04$, $k_{1b}/k_1 = 0.02 \pm 0.02$, and, by difference, $k_{1c}/k_1 = 0.08 \pm 0.04$. The individual rate coefficients obtained from k_1 and the branching fractions are $k_{1a} = (7.8 \pm 1.4) \times 10^{-11}$, $k_{1b} = (2 \pm 2) \times 10^{-12}$, and $k_{1c} = (7 \pm 4) \times 10^{-12}$ cm^3 $molecule^{-1}$ s^{-1}. The errors given include the statistical errors obtained by averaging the individual measurements plus estimates of the experimental error.

Discussion

Computer Simulations. Both the H + HO_2 and the H + NO_2 systems were modeled by using the reactions and rate constants given in Table VI. Because of the uncertainty in OH* yields from H + HO_2 and because many of the rate constants for OH* reactions are poorly known, simulations were used only as an additional check for secondary reactions and to test whether a reasonable model incorporating reactions of OH* could account for the large decrease in atomic oxygen yields from both H + HO_2 and H + NO_2 when quenchers were added.

Since the H + NO_2 reaction is known to produce OH* at yields near 50%,[25,30-34] simulations of this system were used to obtain estimates for several of the OH* rate constants before simulations of the H + HO_2 reaction were attempted. Initial concentrations of atomic hydrogen were varied from 5×10^{12} to 1.5×10^{13} cm^{-3} with initial NO_2 at 1.2×10^{12} cm^{-3}. A yield of 0.5 OH* per NO_2 reacted was used. Rate constants for reactions 33b, 34, and 35 were varied to reproduce the observed atomic oxygen yields in the absence of added water. Experimental yields were best fit for $k_{33b} = 2 \times 10^{-11}$ cm^3 $molecule^{-1}$ s^{-1} and $k_{34} = k_{35} = 1 \times 10^{-10}$ cm^3 $molecule^{-1}$ s^{-1}. Estimated uncertainties in the rate constants are a factor of 5 for k_{33b} and about a factor of 10 for k_{34} and k_{35}. With water added at a concentration of 5×10^{15} cm^{-3}, the best fit to observed atomic oxygen yields was obtained for $k_{36} = 5 \times 10^{-11}$ cm^3 $molecule^{-1}$ s^{-1} with an estimated uncertainty of a factor of 5.

The atomic oxygen yields from H + NO_2 observed in the present study cannot be fit by using the surface reaction of atomic hydrogen with ground-state OH (eq 45, $k_{45} = 3.2 \times 10^{-13}$ cm^3

$$H + OH + \text{wall} \rightarrow O + \text{products} \qquad (45)$$

$molecule^{-1}$ s^{-1}) reported by Glass and Chaturvedi.[36] If reaction 45 is used as the source of atomic oxygen, calculated yields are about a factor of three lower than observed. Moreover, the calculated yields increase strongly with increasing [H] while the observed yields were nearly independent of [H]. Although reaction 45 cannot account for atomic oxygen production in the present study, it would have been considerably more important in the work of Glass and Chaturvedi who used concentrations of NO_2 and

(30) Wickramaaratchi, M. A.; Setser, D. W.; Hildebrandt, B.; Korbitzer, B.; Heydtmann, H. *Chem. Phys.* **1984**, *84*, 105.
(31) Agrawalla, B. S.; Manocha, A. S.; Setser, D. W. *J. Phys. Chem.* **1981**, *85*, 2873.
(32) (a) Murphy, E. J.; Brophy, J. H.; Arnold, G. S.; Dimpfl, W. L.; Kinsey, J. L. *J. Chem. Phys.* **1981**, *74*, 324. (b) Murphy, E. J.; Brophy, J. H.; Kinsey, J. L. *J. Chem. Phys.* **1981**, *74*, 331.
(33) Mariella, R. P., Jr.; Lantzsch, B.; Maxson, V. T.; Luntz, A. C. *J. Chem. Phys.* **1978**, *69*, 5411.
(34) Polanyi, J. C.; Sloan, J. J. *Int. J. Chem. Kinet., Symp. 1* **1975**, 51.
(35) Finlayson-Pitts, B. J.; Kleindienst, T. E.; Ezell, M. J.; Toohey, D. W. *J. Chem. Phys.* **1981**, *74*, 4533.
(36) Glass, G. P.; Chaturvedi, B. K. *Int. J. Chem. Kinet.* **1982**, *14*, 153.

TABLE VI: Reactions Used in Computer Simulations

no.	reaction	rate constant at 300 K[a]
1a	$H + HO_2 \rightarrow OH + OH\ (OH^*)$[b,c]	7.8×10^{-11} [d]
1b	$H + HO_2 \rightarrow O + H_2O$	2.0×10^{-12} [d]
1c	$H + HO_2 \rightarrow H_2 + O_2$	7.0×10^{-12} [d]
2	$OH + OH \rightarrow O + H_2O$	1.9×10^{-12}
3	$O + OH \rightarrow H + O_2$	3.3×10^{-11}
4	$O + HO_2 \rightarrow OH + O_2$	6.1×10^{-11} [e]
5	$OH + HO_2 \rightarrow H_2O + O_2$	6.4×10^{-11} [f]
6	$OH + H_2O_2 \rightarrow HO_2 + H_2O$	1.7×10^{-12}
7	$HO_2 + HO_2 \rightarrow H_2O_2 + O_2$	1.7×10^{-12}
8a	$H + H_2O_2 \rightarrow HO_2 + H_2$	2.0×10^{-14}
8b	$H + H_2O_2 \rightarrow OH + H_2O$	3.0×10^{-14}
9	$H + OH \rightarrow O + H_2$	3.0×10^{-17} [g]
10	$O + H_2O_2 \rightarrow OH + HO_2$	1.7×10^{-15}
11	$OH + H_2 \rightarrow H + H_2O$	6.7×10^{-15}
12	$H + F_2 \rightarrow F + HF$	2.5×10^{-12} [h]
13	$F + H_2 \rightarrow H + HF$	2.7×10^{-11}
14	$F + H_2O_2 \rightarrow HO_2 + HF$	5.0×10^{-11} [i]
15	$F + H_2O \rightarrow OH + HF$	1.1×10^{-11} [i]
16	$F + HO_2 \rightarrow O_2 + HF$	4.0×10^{-11} [j]
17	$F + OH \rightarrow O + HF$	1.5×10^{-11} [j]
18	$OH + wall \rightarrow products$	10 s^{-1} [d]
19	$HO_2 + wall \rightarrow products$	5 s^{-1} [d]
20	$O + wall \rightarrow products$	2 – 10 s^{-1} [k]
21	$HO_2 + NO \rightarrow OH + NO_2$	8.3×10^{-12}
22	$H + NO_2 \rightarrow NO + OH(OH^*)$[b,l]	1.3×10^{-10}
23	$OH + NO + He \rightarrow HONO + He$	3.8×10^{-31} [m]
24	$O + NO + He \rightarrow NO_2 + He$	6.2×10^{-32} [m]
25	$H + NO + He \rightarrow HNO + He$	2.0×10^{-32} [m]
26	$OH + NO_2 + He \rightarrow HONO_2 + He$	9.2×10^{-31} [m]
27	$H + HNO \rightarrow H_2 + NO$	1.0×10^{-13}
28	$O + NO_2 \rightarrow O_2 + NO$	9.3×10^{-12}
29	$O + HONO \rightarrow OH + NO_2$	1.0×10^{-15}
30	$OH + HONO \rightarrow H_2O + NO_2$	6.6×10^{-12}
31	$OH + HNO \rightarrow H_2O + NO$	7.0×10^{-11}
32	$NO + F_2 \rightarrow F + FNO$	1.5×10^{-14} [n]
33a	$OH^* + H \rightarrow OH + H$	3.0×10^{-10} [o]
33b	$OH^* + H \rightarrow O + H_2$	2.0×10^{-11} [k]
34	$OH^* + OH \rightarrow O + H_2O$	1.0×10^{-10} [k]
35	$OH^* + OH^* \rightarrow O + H_2O$	1.0×10^{-10} [k]
36	$OH^* + H_2O \rightarrow OH + H_2O$	5.0×10^{-11} [k]
37a	$OH^* + H_2O_2 \rightarrow OH + H_2O_2$	1.5×10^{-11} [p]
37b	$OH^* + H_2O_2 \rightarrow HO_2 + H_2O$	1.7×10^{-12} [p]
38	$OH^* + O \rightarrow H + O_2$	1.0×10^{-10} [q]
39	$OH^* + HO_2 \rightarrow H_2O + O_2$	6.4×10^{-11} [p]
40	$OH^* + H_2 \rightarrow H + H_2O$	1.0×10^{-14} [p]
41	$OH^* + F \rightarrow O + HF$	1.5×10^{-11} [p]
42	$OH^* + wall \rightarrow products$	50 s^{-1} [o]

[a] Unless otherwise indicated, units are cm^3 $molecule^{-1}$ s^{-1} and values were taken from ref 37–39. [b] OH* represents OH in the $v = 1$, 2, or 3 vibrational level of the ground electronic state. [c] A yield of 0.9 OH* per HO_2 reacted gave the best fit to observed atomic oxygen concentrations without added quenchers, see text. [d] Measured. [e] Reference 13. [f] Reference 15. [g] Reference 40. [h] References 41 and 42. [i] Reference 43. [j] Reference 14. [k] Determined by best fit to experimental product yields. [l] A yield of 0.5 OH* per NO_2 reacted was used in the model. [m] cm^6 $molecule^{-2}$ s^{-1}. [n] Reference 44. [o] Reference 25. [p] Estimated. [q] Reference 45.

atomic hydrogen about a factor of 10 higher than those used here.

The value of k_{33b} obtained here is consistent with the observations of Spencer and Glass[25] that nonreactive quenching (eq 33a) dominates reaction of atomic hydrogen with OH*. The present study cannot tell whether reaction 33b occurs in the gas phase or on the reactor surface but a gas-phase reaction of OH* seems more likely. The result for k_{36} is also in reasonably good agreement with the value of 1.4×10^{-11} cm^3 $molecule^{-1}$ s^{-1} reported by Glass et al.[26]

At the high initial stoichiometric ratios used, secondary reactions are not expected to interfere with the H + HO_2 total rate constant measurements. As an additional check, these experiments were simulated by using the reactions in Table VI. The procedure has been described in detail elsewhere[13] and only the results are summarized here. Initial concentrations of HO_2 were varied from 7.5×10^{11} to 2.5×10^{12} cm^{-3} with initial atomic hydrogen at 1 $\times 10^{11}$ cm^{-3}. A 90% yield of OH* from reaction 1 was assumed (see below). Values of k_1 calculated from the model were within 8% of the input value and confirmed that secondary reactions do not interfere with the present measurements.

Product yields from the H + HO_2 reaction were corrected experimentally for secondary reactions at long reaction times (>5 ms) by extrapolating observed yields to $t = 0$. Computer simulations were carried out to check the validity of this correction procedure and to check for additional interference at short reaction times (<5 ms) due to HO_2 (reactions 4 and 5) and possibly due to vibrationally excited OH* (reactions 33–42). Initial concentrations of atomic hydrogen were varied from 5×10^{12} to 1.5×10^{13} cm^{-3} with initial HO_2 at 5×10^{11} cm^{-3}. Simulations were carried out without added water and with water at 5×10^{15} cm^{-3}. Yields of OH and atomic oxygen calculated over the time interval 6 to 20 ms were extrapolated to $t = 0$. A similar procedure with excess NO was used to determine $[HO_2]_0$. As in the experimental runs, branching fractions were then determined by using eq III and IV. For $[H] > 7.5 \times 10^{12}$ cm^{-3}, calculated values of k_{1a} were within 10% of the model input value with and without added water; this is evidence that the extrapolation to $t = 0$ effectively corrects for secondary reactions occurring in this system. At $[H] = 5 \times 10^{12}$ cm^{-3}, k_{1a} calculated from the model was 20% below the input value. For this reason, one experiment carried out at a low atomic hydrogen concentration was not included in the average reported in Table III. In order to reproduce atomic oxygen observed without added water, the model required a yield of 0.9 OH* per HO_2 consumed by reaction 1 with an estimated uncertainty of a factor of 2. When water was added, k_{1b} calculated from the model agreed with the input value within 15%. This supports the suggestion that vibrationally excited OH is the major source of atomic oxygen observed in the H + HO_2 system without added quenchers.

Comparison with Previous Results. Recent measurements of k_1 near 300 K are summarized in Table VII. Two of the studies obtained k_1 relative to the rate constant for the H + O_2 + M reaction (eq 46) by determining steady-state concentrations of

$$H + O_2 + M \rightarrow HO_2 + M \qquad (46)$$

HO_2.[5,6] Under the experimental conditions used, rate constants (k_{46}) with M = He (or Ar) and with M = O_2 were required in order to obtain k_1. Considering the uncertainties in the reference rate constants, the agreement between the relative measurements and the present study is reasonably good.

The three remaining entries in Table VII were absolute measurements. The results of the present study agree very well with those of Sridharan, Qiu, and Kaufman.[7] In both studies resonance fluorescence (RF) was used to follow the decay of atomic hydrogen in the presence of excess HO_2. Hack, Preuss, and Wagner[5] used laser magnetic resonance (LMR) to follow the decay of HO_2 in excess atomic hydrogen; the results are about 70% below the average of the two RF studies. Secondary reactions in either the LMR or RF studies are not likely explanations of this difference. Computer simulations of the LMR study indicate that H_2O_2 concentrations were sufficiently low that production of HO_2 from OH + H_2O_2 (eq 6) should not lower the observed rate by more than about 10%. Moreover, reaction of HO_2 with product OH from H + HO_2 should not have increased the observed HO_2 loss by more than about 15%. In both RF studies initial concentrations

TABLE VII: Summary of k_1 Measurements near 300 K

$10^{11}k_1$, cm^3 $molecule^{-1}$ s^{-1}	press., Torr	method[a]	comments	ref
6.0 ± 1.7	5.0	LMR	relative to H + O_2 + M	5
4.6 ± 1	1.0	LMR	absolute study [H] >> [HO_2]	5
5.0 ± 1.3	2.5–3.2	LMR	relative to H + O_2 + M	6
7.4 ± 1.2	2.5	RF	absolute study [HO_2] >> [H]	7
8.7 ± 1.5	1.0	RF	absolute study [HO_2] >> [H]	present study

[a] LMR = laser magnetic resonance, RF = resonance fluorescence.

TABLE VIII: Summary of Branching Fraction Measurements for the H + HO_2 Reaction

k_{1a}/k_1 (OH + OH)	k_{1b}/k_1 (O + H_2O)	k_{1c}/k_1 (H_2 + O_2)	method[a]	comments	ref
0.69	0.02	0.29	ESR	add NO; observe changes in [O] and [OH]	12
0.87 ± 0.04	0.04 ± 0.02	0.09 ± 0.045	RF	add H; observe product [OH] and [O]; no OH quenchers added	7
0.90 ± 0.04	0.02 ± 0.02	0.08 ± 0.04	RF	add H; observe product [OH] and [O]; water added to quench OH	present study

[a] ESR = electron spin resonance; RF = resonance fluorescence.

and stoichiometric ratios were such that secondary reactions, even those involving vibrationally excited OH, should not interfere. This was confirmed by the experimental tests and computer simulations discussed above. The reason for the disagreement between the LMR and RF studies is not clear at the present time; it may lie in the combined experimental errors, the largest of which arise from measurements of absolute radical or atomic concentrations.

Recent branching fraction results are summarized in Table VIII. The three studies generally agree that the major reaction pathway is OH production with only a minor contribution from the atomic oxygen channel. Earlier studies have reported widely different values for the branching fractions.[8-11] Potential problems with these studies have been discussed previously[7,46] and these early results will not be considered further here.

In the experiments of Hack, Wagner, and Hoyermann,[12] HO_2 was produced from the H + O_2 + M reaction (eq 46). Electron spin resonance was used to determine atomic oxygen and OH products from H + HO_2. From the increase in atomic oxygen when NO was added, they obtained $k_{1b}/k_1 \leq 0.02$. They also observed an increase in the OH concentration when NO was added and analyzed their data in terms of eq V where the +NO and

$$(k_{1b} + k_{1c})/k_{1a} = ([OH]_{+NO} - [OH]_{-NO})/[OH]_{-NO} \quad (V)$$

−NO subscripts indicate the presence or absence of added NO. To derive eq V one must assume steady-state HO_2 and neglect secondary reactions such as OH + HO_2, O + OH, and O + HO_2. Also [NO] must be sufficiently large that NO + HO_2 dominates H + HO_2. To test the validity of eq V, the experiments of Hack et al. were simulated by using reaction 46 plus the reactions in Table VI. Initial concentrations were those given by Hack et al. in their Figures 3 and 4. Values of del[OH] (the right-hand side of eq V) obtained from the simulations ranged from about 0.3 to 0.2 for reaction times between 3 and 5 ms. Although these calculated del[OH] values are reasonably close to the value of 0.42 observed by Hack et al., they are a factor of 2 to 3 higher than the input value of 0.12 used for $(k_{1b} + k_{1c})/k_{1a}$ (left-hand side of eq V) in the model. Thus, the simulations show that, under the experimental conditions used by Hack et al., eq V cannot be used to obtain branching ratios from observed del[OH]. Equation V fails mainly because of interference from secondary reactions and to a lesser extent because of non-steady-state HO_2. The observed del[OH] can be fit reasonably well by the computer simulations for k_{1a}/k_1 in the range 0.8 to 0.9 and for $(k_{1b} + k_{1c})/k_1$ from 0.2 to 0.1. The experimental observations of Hack et al. are not inconsistent with the RF measurements when allowance is made for the uncertainties involved in fitting the observed del[OH] to a computer model.

In the branching fraction experiments of Sridharan et al.,[7] resonance fluorescence was used to determine the atomic oxygen and OH products of reaction 1 by adding HO_2 to an excess of atomic hydrogen. Data were taken at one reaction time near 4 ms and corrections for secondary chemistry were made by using a combination of separate experimental and computational methods. This is a somewhat different approach than that used in the present study where product data were taken at several reaction times and an internal experimental method was used to correct for secondary reactions. In both studies corrections to observed [OH] were less than 10% and the resulting values for k_{1a}/k_1 are in excellent agreement. For the atomic oxygen channel, Sridharan et al. experimentally corrected for secondary atomic oxygen production from OH + OH by using H + NO_2 to generate OH concentrations equal to those observed in their branching fraction runs. However, as shown above, secondary reactions of vibrationally excited OH are a major source of atomic oxygen production in both the H + NO_2 and the H + HO_2 systems. Since the yield of OH* from H + HO_2 is only poorly known, it is difficult to assess whether the procedure used by Sridharan et al. completely corrects for secondary production of atomic oxygen. In the present study addition of OH quenchers was used to minimize this type of interference. Considering the uncertainties introduced by the large background corrections required in both studies, the agreement between the reported values for k_{1b}/k_1 is reasonably good.

Temperature Dependence. Over the temperature range 245 to 300 K no significant change was observed in either the total rate coefficient or the branching fractions for reaction 1. The large value found for k_{1a}, its approximate independence of temperature over the range studied, and the evidence that vibrationally excited OH is produced are all consistent with the view that this channel proceeds via an energy-rich intermediate complex (H···OOH) which subsequently decomposes to 2 OH.[7] Although no temperature dependence was found for k_{1b}, the low yields of atomic oxygen in the presence of high background concentrations limit the sensitivity of the present method for studying this channel and no firm conclusion on its temperature dependence can be made. Values for k_{1c} were determined by difference in the present study. Because of its importance in atmospheric chemistry, a more direct study of this channel and its temperature dependence is warranted (see Summary section).

Summary

The total rate constant for the H + HO_2 reaction has been measured by the discharge flow technique. The result is (8.7 ± 1.5) × 10^{-11} cm^3 $molecule^{-1}$ s^{-1}, independent of temperature between 245 and 300 K.

Product yields of OH and atomic oxygen from H + HO_2 were measured directly by using resonance fluorescence detection. Addition of water vapor to the system reduced atomic oxygen production significantly but had little or no effect on OH yields. Reaction of OH with excess CO also lowered observed yields of atomic oxygen in this system. A similar reduction of oxygen atom yields was observed when the same quenchers were added to the

(37) DeMore, W. B.; Margitan, J. J.; Molina, M. J.; Watson, R. T.; Golden, D. M.; Hampson, R. F.; Kurylo, M. J.; Howard, C. J.; Ravishankara, A. R. Jet Propulsion Laboratory: California Institute of Technology, Pasadena, CA, 1985; JPL Publication No. 85-37.
(38) Baulch, D. L.; Cox, R. A.; Hampson, R. F., Jr.; Kerr, J. A.; Troe, J.; Watson, R. T. *J. Phys. Chem. Ref. Data* **1984**, *13*, 1259.
(39) Hampson, R. F. Federal Aviation Administration Report No. FAA-EE-80-17, 1980, Washington, DC.
(40) Kerr, J. A.; Moss, S. J. *CRC Handbook of Bimolecular and Termolecular Gas Reactions*, Vol. II; Chemical Rubber Co.: Cleveland, OH, 1981.
(41) Goldberg, I. B.; Schneider, G. R. *J. Chem. Phys.* **1976**, *65*, 147.
(42) Homann, K. H.; Schweinfurth, H.; Warnatz, J. *Ber. Bunsenges. Phys. Chem.* **1977**, *81*, 724.
(43) Walther, C. D.; Wagner, H. Gg. *Ber. Bunsenges. Phys. Chem.* **1983**, *87*, 403.
(44) Kolb, C. E. *J. Chem. Phys.* **1976**, *64*, 3087.
(45) Spencer, J. E.; Glass, G. P. *Int. J. Chem. Kinet.* **1977**, *9*, 111.
(46) Lloyd, A. C. *Int. J. Chem. Kinet.* **1974**, *6*, 169.

$H + NO_2$ reaction which is known to produce vibrationally excited OH with high efficiency. This is evidence that most of the atomic oxygen observed in both systems without added quenchers was not formed as a primary product but rather was produced from secondary reactions of vibrationally excited OH. The $H + HO_2$ product yields reported here are those observed with added water vapor. The resulting branching fractions are $k_{1a}/k_1 = 0.90 \pm 0.04$ and $k_{1b}/k_1 = 0.02 \pm 0.02$. The rate constants are $k_{1a} = (7.8 \pm 1.4) \times 10^{-11}$ cm^3 molecule^{-1} s^{-1} and $k_{1b} = (2 \pm 2) \times 10^{-12}$ cm^3 molecule^{-1} s^{-1}, independent of temperature between 245 and 300 K.

The branching fraction for channel c was obtained by difference using the measured values given above for channels a and b. The results are $k_{1c}/k_1 = 0.08 \pm 0.04$ and $k_{1c} = (7 \pm 4) \times 10^{-12}$ cm^3 molecule^{-1} s^{-1}. This product channel is an important source of molecular hydrogen in the mesosphere.[2,4] Moreover, recent mesospheric model results[1] show that calculated ozone concentrations near the mesopause (80 km) are very sensitive to the magnitude of k_{1c}. Thus, a more direct measurement of this rate constant would be of value in understanding the HO_x chemistry of the upper atmosphere.

Acknowledgment. The research described in this paper was performed at the Jet Propulsion Laboratory, California Institute of Technology, under contract with the National Aeronautics and Space Administration.

CONDENSED PHASES AND MACROMOLECULES

SO_2^- Doping of $SrTiO_3$ and $SrZrO_3$ by Cyclic (CS_2–O_2) Processing

Michiko Yonemura, Tadao Sekine, and Hisashi Ueda*

National Chemical Laboratory for Industry, Tsukuba Research Center, Yatabemachi, Ibaraki 305, Japan
(Received: August 6, 1985)

The heating of $SrTiO_3$ or $SrZrO_3$ alternately in CS_2 (800 °C) and O_2 (600 °C) has been demonstrated as a method for the introduction of SO_2^- dopant ions. When this heating cycle is repeated several times, a paramagnetic species having g factor components of 2.0069, 2.0115, and 2.0021 is generated in these compounds. This species is identified as SO_2^-. The formation of SO_2^- in these wide band gap semiconductors adds a visible light response to them.

The anion radical SO_2^- has been studied by ESR in both liquid solutions and solid matrices, It is formed in solutions as hydrolysis product when $Na_2S_2O_4$ is dissolved in water[1-5] or by electrolytic reduction in solutions of SO_2 in dimethylformamide.[6,7] In solids it is formed upon γ- or X-irradiation of sulfur-containing compounds, such as $Na_2S_2O_4$ or $K_2S_2O_5$,[2] and alkali halides doped with SO_2.[8] Satellite lines due to ^{33}S ($I = {}^3/_2$), natural abundance 0.74%, have been detected in both aqueous solution[2,5] and in γ-irradiated alkali halides doped with SO_2.[8]

It has been found by the present authors that when $SrTiO_3$ or $SrZrO_3$ is repeatedly heated in CS_2 at 800 °C and then in O_2 at 600 °C, and this heating cycle repeated more than 3 times, these materials partly change their electronic structure to absorb visible light and also to possess some photocatalytic activity.[9] Both of these treated compounds exhibit ESR absorption in the g factor region of 2.00–2.02. Therefore, the purpose of the present paper is to find if the ESR absorption thus found in treated $SrTiO_3$ and $SrZrO_3$ can be ascribed to SO_2^-. It is desirable to know the significance of SO_2^- doping in these crystals.

Experimental Section

$SrTiO_3$, polycrystalline, was obtained from Mitsuwa Rikagaku Co., 99.9%. $SrTiO_3$, single crystal, was obtained from Nakazumi Earth Crystal Co., 2 mm thickness, cut parallel to the (100) plane. $SrZrO_3$, polycrystalline, was prepared by heating a 1:1 mixture of $SrCO_3$ and ZrO_2 at 1200 °C for 2 h. CS_2 processing was done by heating in CS_2 vapor at 13.3 Pa and at 800 °C for 1 h. O_2 processing was done by heating in O_2 at 0.1 MPa and at 600 °C for 1 h. CS_2 processing followed by O_2 processing was repeated 4–6 times. The final processing cycle was made at lower temperatures: CS_2 at 500 °C and O_2 at 300 °C. ESR measurements were carried out using a JES ME3X type spectrometer using 100-kHz magnetic field modulation and at 20 °C.

In Figure 1 the ESR spectrum obtained from the polycrystalline $SrTiO_3$ and $SrZrO_3$ after six cycles of CS_2–O_2 processing is shown. The g factor values were determined by using diphenylpicrylhydrazyl ($g = 2.0036$) and the spacing of the central two lines of Mn^{2+} ESR absorption lines (8.67 mT). In Figure 2 the ESR spectrum of the photocatalyst prepared from $SrTiO_3$ which has been modified by CS_2–O_2 cycles and has been used for photocatalytic reactions is shown. The ΔH_{msl} value of the central component is 0.19 mT while the value for the spectra in Figure 1 is 0.09 mT. Through some ESR absorption is observed from untreated $SrTiO_3$ or $SrZrO_3$, no ESR absorption having line widths comparable to those in Figure 1 has been found in either case. The ESR spectrum from the single crystal of $SrTiO_3$ after four cycles of CS_2–O_2 processing did not indicate the presence

(1) Clark, H. C.; Horsfield, A.; Symons, M. C. R. *J. Chem. Soc.* **1961**, 7.
(2) Atkins, P. W.; Horsfield, A.; Symons, M. C. R. *J. Chem. Soc.* **1964**, 5220.
(3) Pinker, R. G.; Gordon, T. P.; Mason, D. M.; Corcoran, W. H. *J. Phys. Chem.* **1959**, *63*, 302.
(4) Lynn, S.; Pinker, R. G.; Corcoran, W. H. *J. Phys. Chem.* **1964**, *68*, 2363.
(5) Burlamacchi, L. *Mol. Phys.* **1969**, *16*, 369.
(6) Dinse, K. P.; Möbius, K. *Z. Naturforsch., A* **1968**, *23A*, 695.
(7) Pinker, R. G.; Lynn, S. *J. Phys. Chem.* **1968**, *72*, 4706.
(8) Schneider, J.; Dichler, N.; Rauver, A. *Phys. Status Solidi* **1966**, *13*, 141.
(9) Sekine, T.; Ueda, H.; Yonemura, M. *Nippon Kagaku Kaishi* **1985**, 1024.

0022-3654/86/2090-3003$01.50/0